Influence of Higher Order Modes on the Measurements of Complex Permittivity and Permeability of Materials Using a Microstrip Discontinuity

Patrick Quéffélec and Philippe Gelin

Abstract—**The accurate electromagnetic analysis of discontinuities in a microstrip device, used for the broad band measurement of complex permittivity and permeability of materials, is presented. This analysis is based on the spectral domain approach together with the mode matching method which consists in the electromagnetic field matching at the discontinuities for each mode of the microstrip line. The study of the influence of higher order modes on the S-parameter measurements enabled us to determine the domain of validity of the transmission-line theory that has been used until now in the processing of the data. The use of the transmission-line theory for the description of the electromagnetic behavior of the cell discontinuities permits in the 45 MHz-14 GHz frequency band the achievement of a good precision (better than 5%) for the results on materials with low electromagnetic characteristics ($\varepsilon' < 10$ and $\mu' < 10$). The improvement in high frequencies of the results on materials with greater permittivity and permeability is provided by the calculation of higher order modes (about 10) in the analysis of the microstrip discontinuity.**

I. Introduction

A BROAD BAND (45 MHz–14 GHz) measurement method for complex permittivity $\varepsilon^* = \varepsilon' - j\varepsilon''$ and permeability $\mu^* = \mu' - j\mu''$ of materials has previously been set out [1]. This method, inspired from Weir's works [2] and from Barry's ones [3], is based on the reflection/transmission measurement of a microstrip line loaded with the test sample (Fig. 1). Indeed, the measurement results obtained by this technique for low loss materials (typically $\varepsilon'' < 0.1$ and $\mu'' < 0.1$) are less precise than those obtained by a method using a cavity resonator [4], because of the impedance mismatching of the transmission line. Yet, the use of a thru-reflect-line (TRL) calibration procedure [5] for the network analyzer permits increasing the sensitivity of the method. In fact, the main interest of the reflection/transmission technique is the broadness of the useful frequency band, opening up new prospects for applications such as microwave electromagnetic compatibility (EMC), that calls for the broad band electromagnetic characterization of lossy materials.

Manuscript received April 9, 1995; revised February 15, 1996. This work was supported by the Direction des Recherches Etudes et Techniques (Délégation Générale de l'Armement) under Contract 93/2516A.

P. Quéffélec is with LEST (URA CNRS no. 1329), Université de Bretagne Occidentale, U.F.R. Sciences, BP 809, 29285 Brest Cedex, France.

P. Gelin is with LEST, ENST de Bretagne, 29285 Brest Cedex, France.

Publisher Item Identifier S 0018-9480(96)03809-4.

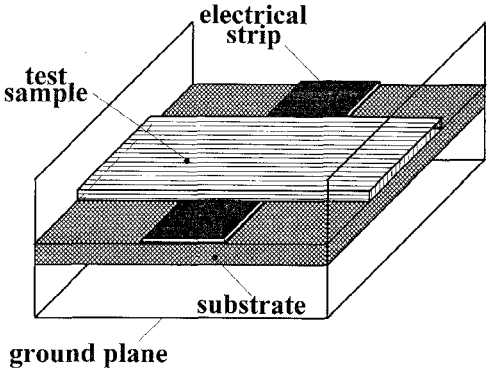

Fig. 1. Microstrip cell loaded with the sample under test.

To obtain ε^* and μ^* of the material from the S-parameter measurements, it is necessary to use an accurate electromagnetic analysis of the test device (direct problem) together with an optimization program (inverse problem). The direct problem corresponds to the calculation of the S-parameters of the test device as functions of the complex permittivity and permeability of the material present in the cell. This broad band calculation requires a full-wave analysis: the spectral domain approach (SDA) [6]–[8] for the electromagnetic characterization of the microstrip line, and the study of cell discontinuities (unloaded/loaded line discontinuities). The first approach chosen in the discontinuities analysis was the transmission-line theory [1]. This theory consists in taking only the dominant hybrid mode propagated in each region of the cell into account, neglecting the higher order modes that can be excited at the discontinuities.

The broad band measurement method that was developed, when fitted out with a TRL calibration procedure for the network analyzer enabled us to characterize homogeneous or heterogeneous dielectrics and magnetic materials with low electromagnetic characteristics (typically $\varepsilon' < 10$ and $\mu' < 10$ over about 6 GHz) with a good precision in the 500 MHz-14 GHz frequency band. In general, the results are accurate to better than 5% for these materials. Fig. 2 and Fig. 3 illustrate these results for a composite material (polymer and carbon black) and a NiZn ferrite. Concerning the composite, the measured ε^* data of $3.7 - j0.1$ agrees with the results

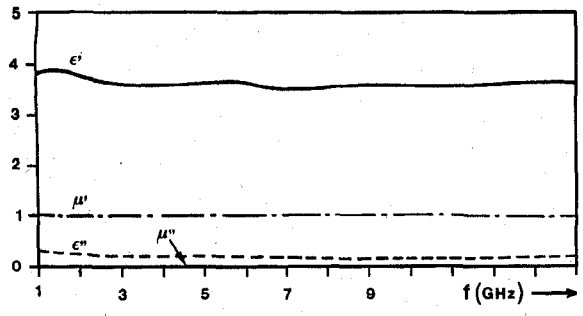

Fig. 2. Measured ε^* and μ^* data for a composite material (polymer and carbon black).

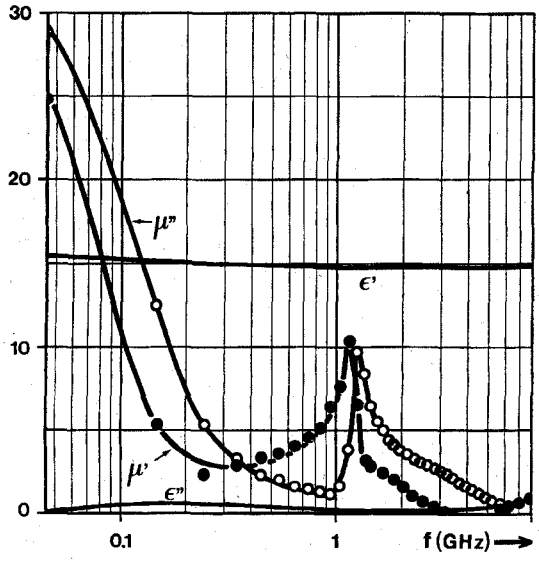

Fig. 3. Measured ε^* and μ^* data for a NiZn ferrite.

obtained by other laboratories using standard characterization techniques (cavity, guide). As would be expected $\mu^* = 1 - j0$ was measured. The measured ε^* data of $15 - j0.5$ for the ferrite agrees with the results obtained at low frequencies with another method. The measured μ^* data is in close agreement with the results given in literature [9]. At high frequencies the results are less precise for the materials with a higher value of permittivity and permeability. For example, Fig. 4 shows the measured ε^* and μ^* data for a dielectric with a high dielectric constant. The value of the permittivity is constant ($\varepsilon' = 30$) in the exploited frequency band, whereas the measured ε' data decreases when the frequency increases. The analysis of the error sources depending of our measurement method has been previously made [1]. In order to explain the decreasing of the accuracy of the results at high frequencies for materials with a high permittivity and/or permeability, the error analysis brought us to put the problem of the domain of validity of the transmission-line theory that has been used until now in the studying of the measurements and in which the higher order modes are neglected.

In this paper we will present the accurate electromagnetic analysis of the microstrip cell discontinuities in order to show the influence of the microstrip line higher order modes on the measurement results.

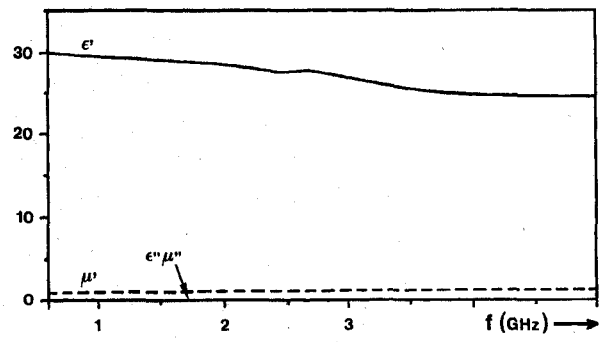

Fig. 4. Measured ε^* and μ^* data for a ceramic.

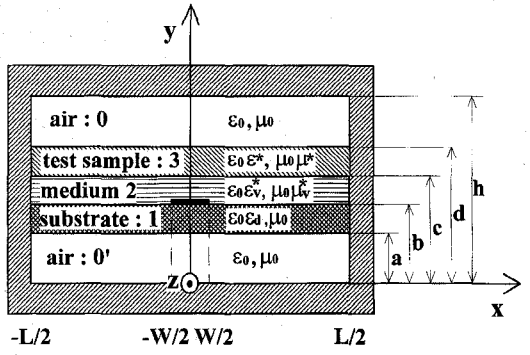

Fig. 5. Microstrip line cross section.

II. Electromagnetic Description of the Test Device

The rigorous description of the electromagnetic behavior of the cell discontinuities calls for the taking into account of the maximum of physical phenomena in the model used. In the cell, the dominant mode of the microstrip line interacts with the unloaded/loaded line discontinuities. So, part of the energy transported by this mode is reflected and transmitted in the line, i.e., reflection and transmission of the dominant mode and excitation of propagated higher order modes, and the other part is stored in the neighborhood of each discontinuity. The stored energy corresponds to the excitation of evanescent higher order modes. The spectral domain approach used for the microstrip line electromagnetic analysis is not restrictive for this type of analysis but allows us to take all the modes present in the microstrip cell into account. The problem is essentially the location of the zeros of a characteristic equation and then to match the electromagnetic fields at the discontinuities for each mode.

In this paper, we will first describe the electromagnetic analysis of the microstrip line treated by the spectral domain approach then we will focus our attention on the study of the cell discontinuities based on the mode matching method [10], [11]. Finally, we will compare the numerical results with measurements to confirm our calculations.

III. Electromagnetic Analysis of the Microstrip Line

The cross section of the transmission line studied here is shown in Fig. 5. It is composed of a boxed microstrip line which corresponds to the cell and a sample under test. We also take into account an air gap between the sample and the

line substrate. The central conductor is assumed to have ideal conductivity and negligible thickness.

A. Electromagnetic Fields in the Microstrip Structure

The spectral domain approach is based on the Fourier expansion of electric and magnetic fields. The Helmholtz equation in each of the layers $i = 1, 2 \cdots 5$ of the circuit medium is

$$(\Delta + \omega^2 \varepsilon_0 \mu_0 \varepsilon_i \mu_i) \begin{Bmatrix} \vec{E}_i \\ \vec{H}_i \end{Bmatrix} = \vec{0}$$

where ε_i is the relative permittivity of the layer, μ_i the relative permeability of the layer, ε_0 the permittivity of free space, μ_0 the permeability of free space, Δ the Laplacian of a vector and ω the wave pulsation.

The solutions of this equation in the propagation direction are

$$E_{zi} = \psi_i^e(x, y,) \exp(-\gamma z) \quad \text{electric field}$$
$$H_{zi} = \psi_i^h(x, y) \exp(-\gamma z) \quad \text{magnetic field}$$

where γ is the propagation constant in the positive z direction.

The propagation constant is defined as

$$\gamma = \alpha + j\beta$$

where α is the attenuation constant and β the phase constant.

The studied structure is symmetrical about the y axis; this permits separating the even modes from the odd modes. The dominant mode of the microstrip line is the first even mode. Since the microstrip discontinuities are also symmetrical about the y axis, we will study the even modes and use the inverse Fourier transforms given by

$$\psi_i^e(x, y) = \sum_{m=+1}^{+\infty} \tilde{\psi}_i^e(\alpha_m, y) \cos \alpha_m x \quad \text{(even function)}$$
$$\psi_i^h(x, y) = \sum_{m=+1}^{+\infty} \tilde{\psi}_i^h(\alpha_m, y) \sin \alpha_m x \quad \text{(odd function)} \quad (1)$$

The values of the spectral variable α_m which also corresponds to the propagation constant in the x direction are chosen in such a way that the boundary conditions on the lateral shields parallel to the y axis are satisfied, i.e.,

$$\alpha_m = (2m - 1)\frac{\pi}{L}. \qquad m = 1, \cdots, \infty$$

where L is the structure length.

The transformed waves potentials $\tilde{\psi}_i^e$ and $\tilde{\psi}_i^h$ can be determined analytically in each of the layers of the circuit medium by solving the Helmholtz equation applied in the transform domain. The boundary conditions prevail for $\tilde{\psi}_i^e$ and $\tilde{\psi}_i^h$ identical to those for the transformed components $\tilde{E}_{y_i}$ and $\tilde{H}_{y_i}$. In a circuit medium of five layers (Fig. 3), the total electromagnetic field can be described by 16 independent spectral distributions $A(\alpha_m), B(\alpha_m), \cdots P(\alpha_m)$. For the interfaces between the different layers, exactly the same number of continuity conditions for the tangential components of the electric and magnetic fields can be formulated in the spectral domain, i.e.,

$$\tilde{E}_{x_i} - \tilde{E}_{x_{i+1}} = 0 \qquad \tilde{E}_{z_i} - \tilde{E}_{z_{i+1}} = 0$$
$$\tilde{H}_{x_i} - \tilde{H}_{x_{i+1}} = \tilde{J}_{z_i} \qquad \tilde{H}_{z_i} - \tilde{H}_{z_{i+1}} = -\tilde{J}_{x_i} \quad (2)$$

for $i = 1, \cdots 4$ and y fixed at its interface value for each subscript i. In interfaces which do not contain conductors, J_{x_i} and J_{z_i} are defined to be zero. The structure studied contains one conductor. This conductor is the strip between layer 1 and layer 2 (Fig. 5). The spectral domain current density components in the strip are denoted $\tilde{J}_x$ and $\tilde{J}_z$. By analytical processing of the relations (2), all the unknown distributions $A(\alpha_m), \cdots P(\alpha_m)$ can be eliminated or expressed by $\tilde{J}_x$ and $\tilde{J}_z$. Finally, the relations (2) reduce to a simpler form

$$\begin{bmatrix} \tilde{E}_x(\alpha_m, y = b) \\ \tilde{E}_z(\alpha_m, y = b) \end{bmatrix} = \begin{bmatrix} L_{11}(\alpha_m) & L_{12}(\alpha_m) \\ L_{21}(\alpha_m) & L_{22}(\alpha_m) \end{bmatrix} \cdot \begin{bmatrix} \tilde{J}_x(\alpha_m, y = b) \\ \tilde{J}_z(\alpha_m, y = b) \end{bmatrix} \quad (3)$$

where $\tilde{E}_x, \tilde{E}_z$ are the electric field components in the plane of the circuit metalization and L is the spectral domain Green's matrix of the microstrip structure.

The matrix equation (3) can be solved by the moment method. The moment method used is the GALERKIN method [12].

B. Applying the Galerkin Method

The Galerkin method consists in expanding one of the unknown components of (3) into a suitable set of basis functions. We expand the surface current densities J_x and J_z, since J_x and J_z are easier to describe in physical terms than the electric field components E_x and E_z. We can write in the space domain

$$J_x(x, y = b) = \sum_{p=1}^{P} c_p J_{xp}(x) \quad (4)$$

$$J_z(x, y = b) = \sum_{q=1}^{Q} d_q J_{zq}(x) \quad (5)$$

where P and Q are respectively the number of basis functions used to describe J_x and J_z, and c_p and d_q are unknown coefficients.

In the plane of the circuit metalization, the electric field is defined to be zero in the strip, and the surface current density only exists in the strip. As a consequence, the scalar products given by

$$\langle J_{xp}(x, y = b), E_x(x, y = b) \rangle = \int_{-L/2}^{+L/2} J_{xp} \cdot E_x \, dx \qquad p = 1, \cdots, P$$
$$\langle J_{zq}(x, y = b), E_z(x, y = b) \rangle = \int_{-L/2}^{+L/2} J_{zq} \cdot E_z \, dx \qquad q = 1, \cdots, Q$$

are equal to zero. Parseval's theorem enables us to write these scalar products in the spectral domain

$$\sum_{m=1}^{\infty} \tilde{J}_{xp}(\alpha_m, y=b) \cdot \tilde{E}_x(\alpha_m, y=b) = 0 \qquad p = 1, \cdots, P \tag{6}$$

$$\sum_{m=1}^{\infty} \tilde{J}_{zq}(\alpha_m, y=b) \cdot \tilde{E}_z(\alpha_m, y=b) = 0 \qquad q = 1, \cdots, Q. \tag{7}$$

Taking (6), (7) and using (3), (4), (5), we get a set of simultaneous equations from which the unknown coefficients c_p and d_q can be found

$$\begin{bmatrix} [K_{ip}^{11}] & [K_{iq}^{12}] \\ [K_{jp}^{21}] & [K_{jq}^{22}] \end{bmatrix} \begin{bmatrix} c_p \\ d_q \end{bmatrix} = [0] \tag{8}$$

where $[K_{ip}^{11}], \cdots, [K_{jq}^{22}]$ are matrices, the elements of which are given by

$$K_{ip}^{11} = \sum_{m=1}^{\infty} \tilde{J}_{xi}(\alpha_m) L_{11}(\alpha_m) \tilde{J}_{xp}(\alpha_m) \qquad i = 1, \cdots, P; p = 1, \cdots P$$

$$K_{iq}^{12} = \sum_{m=1}^{\infty} \tilde{J}_{xi}(\alpha_m) L_{12}(\alpha_m) \tilde{J}_{zq}(\alpha_m) \qquad j = 1, \cdots, P; q = 1, \cdots Q$$

$$K_{jp}^{21} = \sum_{m=1}^{\infty} \tilde{J}_{zj}(\alpha_m) L_{21}(\alpha_m) \tilde{J}_{xp}(\alpha_m) \qquad j = 1, \cdots, Q; p = 1, \cdots P$$

$$K_{jq}^{22} = \sum_{m=1}^{\infty} \tilde{J}_{zj}(\alpha_m) L_{22}(\alpha_m) \tilde{J}_{zq}(\alpha_m) \qquad j = 1, \cdots, Q; q = 1, \cdots Q$$

The electromagnetic characterization of the microstrip structure requires solving (8).

C. Modal Characterization of the Structure

1) Convergence Problems: At this stage of the analysis, the formulation of the electromagnetic problem is rigorous. Yet, the numerical computation calls for, on the one hand, the choice of a finite number of basis functions to describe the current densities in the strip and, on the other hand, the truncation of the Fourier expansions.

It has been shown [13] that if the basis functions used to describe the current densities in the strip contain the correct edge singularity, then accurate results for the propagation coefficients are obtained by using very few terms. The basis functions which have been selected here are the sine and cosine functions. These functions enable us to describe the edge effects in the strip and the parity properties of modes. Moreover, the Fourier transforms of the sine and cosine functions are easily calculated. We have studied the convergence of the propagation coefficients as a function of number of basis functions. This study [14] has shown that accurate results for the propagation constant of the dominant mode are obtained by using only a single term in the x direction and two terms in the z direction.

The following empirical criterion has been put forward [15], [16] to get accurate results when the Fourier expansions are truncated

$$M_{\max} = (KNL)/W \tag{9}$$

where $M_{\max}$ is the number of harmonics in the Fourier expansions, N the number of basis functions, L the structure width, W the strip width and K a coefficient contained between 1 and 1.5.

The study of the convergence of the calculated propagation coefficients as the number of harmonics appearing in the Fourier expansions has permitted us to validate this criterion [14]. We can typically truncate the Fourier expansion after about 100 harmonics for the microstrip structures studied.

2) Optimization of the Spectral Domain Approach by Making Use of Asymptotic Expansions: The dispersion relation linking the frequency to the propagation constant for each mode is given by the equation

$$\det[K] = 0. \tag{10}$$

The location of a zero of this equation calls for the calculation of the matrix K in the complex plane many times. Moreover, the convergence of the calculated value of $\det[K]$ requires to take a large number of harmonics in the Fourier expansions. The computations can be speeded up by making use of asymptotic forms of the spectral domain Green's matrix L [17]. The method consists in expressing the elements of the matrix K as follows:

$$K_{11}^{11} = \sum_{m=1}^{nr} \tilde{J}_{x1}(\alpha_m)(L_{11}(\alpha_m) - H_{11})\tilde{J}_{x1}(\alpha_m) + \sum_{m=1}^{\infty} \tilde{J}_{x1}(\alpha_m) H_{11} \tilde{J}_{x1}(\alpha_m)$$

$$K_{1n}^{12} = \sum_{m=1}^{nr} \tilde{J}_{x1}(\alpha_m)(L_{12}(\alpha_m) - H_{12})\tilde{J}_{zn}(\alpha_m) + \sum_{m=1}^{\infty} \tilde{J}_{x1}(\alpha_m) H_{12} \tilde{J}_{zn}(\alpha_m) \qquad n = 1, 2$$

$$K_{N1}^{21} = \sum_{m=1}^{nr} \tilde{J}_{zN}(\alpha_m)(L_{21}(\alpha_m) - H_{11})\tilde{J}_{x1}(\alpha_m) + \sum_{m=1}^{\infty} \tilde{J}_{zN}(\alpha_m) H_{21} \tilde{J}_{x1}(\alpha_m) \qquad N = 1, 2$$

$$K_{Nn}^{22} = \sum_{m=1}^{nr} \tilde{J}_{zN}(\alpha_m)(L_{22}(\alpha_m) - H_{22})\tilde{J}_{zn}(\alpha_m) + \sum_{m=1}^{\infty} \tilde{J}_{zN}(\alpha_m) H_{22} \tilde{J}_{zn}(\alpha_m) \qquad N = 1, 2 \text{ and } n = 1, 2$$

where

$$H_{11} = \lim_{m\to\infty} L_{11}(\alpha_m)$$
$$H_{12} = \lim_{m\to\infty} L_{12}(\alpha_m)$$
$$H_{21} = \lim_{m\to\infty} L_{21}(\alpha_m)$$
$$H_{22} = \lim_{m\to\infty} L_{22}(\alpha_m).$$

The asymptotic limits $H_{11}, H_{12}, H_{21}, H_{22}$ of the elements of the spectral domain Green's matrix L have finite values since $L_{11}, L_{12}, L_{21}, L_{22}$ (tangent and cotangent functions) converge as m approaches infinity. The matrix K can be written as follows:

$$[K] = \sum_{m=1}^{nr} [D(m)] + \sum_{m=1}^{\infty} [H(m)].$$

The convergence of the first sum is very fast since we can typically truncate it after about ten terms to ensure accuracy. So the reduction in the computation time depends on the form of the matrix H. The second sum can be written in the form

$$\sum_{m=1}^{\infty} [H(m)] = F_1(\omega,\gamma) \cdot \sum_{m=1}^{\infty} [F_2(m)].$$

The matrix F_2 depends only on the ratio of the strip and structure widths. The advantage of this formulation lies in the fact that the matrix F_2 only needs to be calculated once for each microstrip geometry to be considered. Moreover, this summation has the same value for the microstrip line loaded with the sample under test as that for the unloaded microstrip line. This saving is important for the analysis of the cell discontinuities.

Fig. 6 shows that with the asymptotic expansions, the convergence of the propagation constant of the dominant mode as the number of terms taken in the Fourier expansion is increased very fast. Without the asymptotic expansions, the convergence is relatively slow.

The field pattern of the microstrip line is obtained by the calculation of the eigenvector $\vec{V}$ given by

$$\vec{V} = \begin{bmatrix} c_1 \\ d_1 \\ d_2 \end{bmatrix}$$

where c_1, d_1 and d_2 are the weight factors of the basis functions selected to describe the current densities in the strip.

The eigenvector $\vec{V}$ is found by solving the following matrix system

$$\begin{bmatrix} c_1 \\ d_2 \end{bmatrix} = -\begin{bmatrix} K_{11}^{11} & K_{12}^{12} \\ K_{21}^{21} & K_{22}^{22} \end{bmatrix}^{-1} \cdot \begin{bmatrix} K_{11}^{12} \\ K_{21}^{22} \end{bmatrix} \cdot d_1$$

where d_1 is fixed since the determinant of the matrix K is equal to zero for each eigenvalue (redundance of one equation).

The calculation of the weight factors c_1, d_1 and d_2 permits to find the current in the strip. By taking (3), we get the electric field in the plane of the circuit metalization. Finally, by using the continuity conditions we have the total electromagnetic field in the structure.

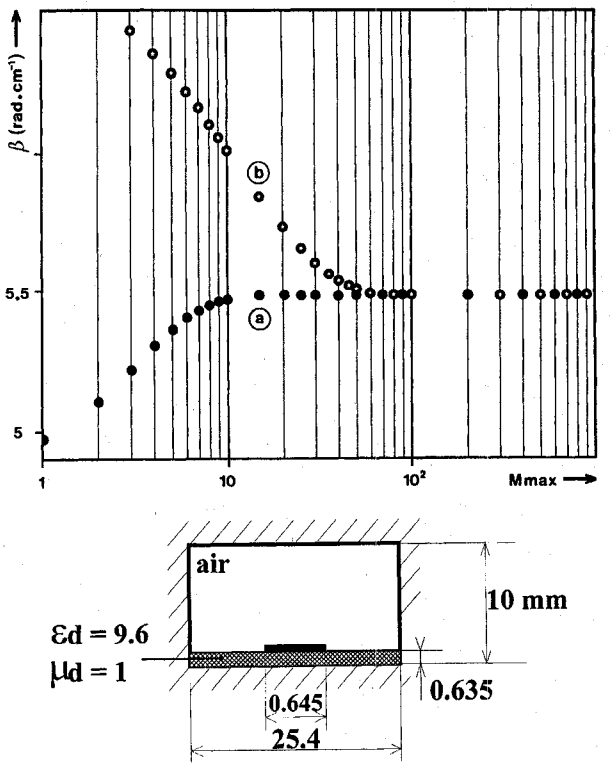

Fig. 6. Convergence of the propagation constant of the dominant mode as the number of terms taken in the Fourier expansions (frequency = 10 GHz). (a) With the asymptotic expansions. (b) Without the asymptotic expansions.

IV. Characterization of the Cell Discontinuities by Modal Analysis

The modal analysis [10], [11] consists in matching the electromagnetic fields at the studied discontinuity for each mode of the structure. The transverse fields are normalized over the cross section of the structure, this permits getting the coupling coefficients between modes and the values of the reflection and transmission coefficients of the discontinuity. So, this method calls for the accurate location of a large number of modes on both sides of the discontinuity.

A. Location of the Modes of the Microstrip Line

The dispersion relation linking the frequency to the propagation constant for each mode is obtained by the location of the complex roots of the characteristic equation of the microstrip line (10). Yet, the calculation of higher order modes is much more difficult than the calculation of the dominant mode because the characteristic equation of the microstrip line also contains many poles that are sometimes very close to the zeros corresponding to the higher order modes. That is why care must be taken not to miss solutions. Fig. 7 shows the typical plot of $\det[K]$ as a function of γ^2.

It has been shown [17] that the poles of (10) correspond to the roots of the dispersion equation of a loaded waveguide which have the same geometry and the same layers as the studied microstrip line. The roots of the dispersion equation of the waveguide correspond to the LSE and LSM modes. In a first time, the accurate location of the modes of the microstrip line was achieved by using the Müller's method [18], [19]

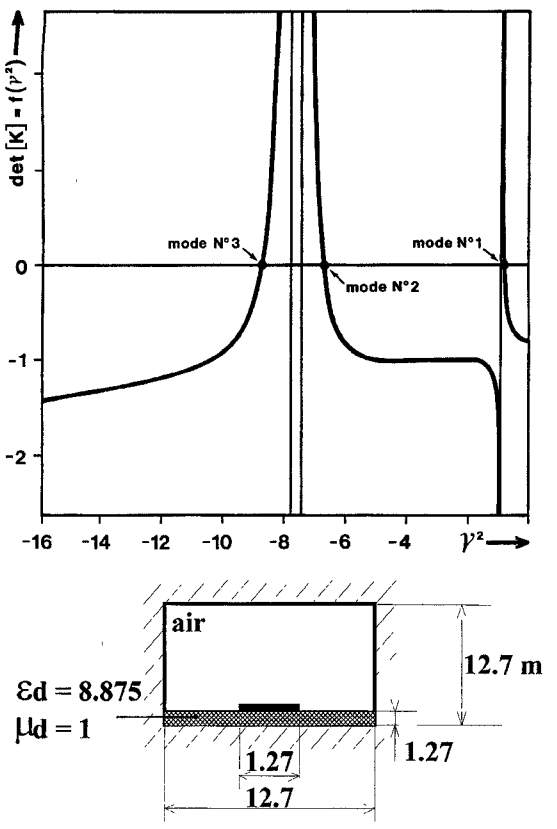

Fig. 7. Typical plot of $\det[K]$ as a function of γ^2 (frequency = 10 GHz).

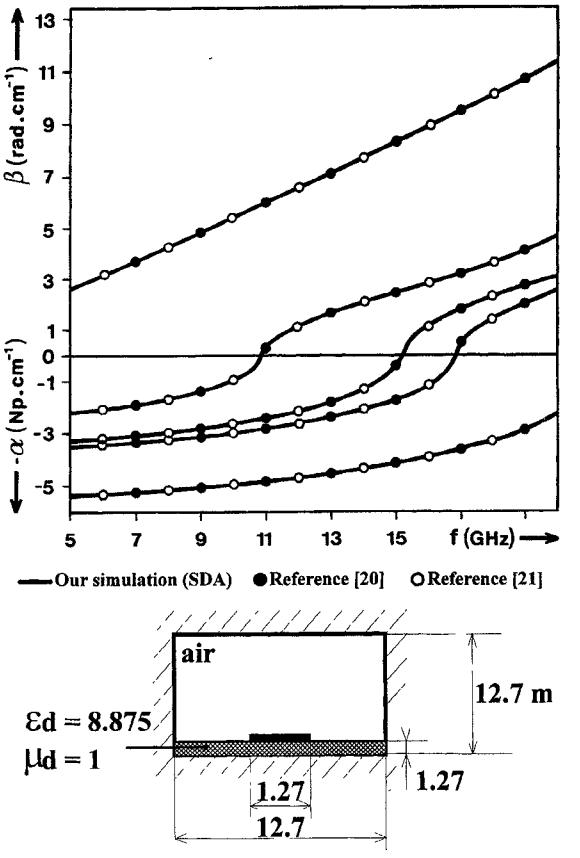

Fig. 8. Dispersion diagram of a typical microstrip line.

and initializing each searched root at the poles calculated by the electromagnetic analysis of the loaded waveguide. Yet, in spite of all the precautions taking during the initialization of the roots, the Müller's method can miss solutions. In this case, the use of a dichotomic method permits to solve (10) on the real axis neglecting the losses of the structure, and finally the location of each root in the complex plane is accomplished by introducing the losses progressively in the calculation. This procedure requires a knowledge of the values of the losses in the studied structure, i.e. the losses of the material under test. Unfortunately, we cannot proceed in such a way in our case because the electromagnetic characteristics of the material are the unknowns of the problem (we want to measure the complex permittivity and permeability of a test sample by solving an inverse problem). As a consequence, the calculation of higher order modes at the time of the resolution of the inverse problem requires the use of a numerical method really suited to the location of complex roots that are very close to the poles of the characteristic equation. We are now developing an expansion in the complex plane of the dichotomic method, usually used for the location of real roots. This study will be published in a next paper. In the present paper, we only consider the calculation of higher order modes in the direct problem, showing the influence of these modes on the S-parameters for a given material in the cell.

We have compared our numerical results to those of the literature to confirm the validity of the calculation of the higher order modes of the microstrip line. Fig. 8 shows that our results are in close agreement with the results given in the literature. The accurate calculation of the higher order modes does not require the increase in the number of basis functions used in the spectral domain approach to describe the current densities in the strip.

After the accurate calculation of the modes of the multilayer microstrip line, we have to match the transverse electromagnetic fields for each mode at the unloaded/loaded line discontinuities in order to get the reflection and transmission coefficients of the microstrip cell.

B. Modal Matching at the Cell Discontinuities

The calculation of the coupling coefficients between modes ρ_n, t_n, R_n, T_n at the unloaded/loaded line discontinuities (Fig. 9) requires four equations. These equations are the continuity conditions for the electric and magnetic fields components in the plane of each discontinuity given by

$z = 0$

$$(1+\rho_0)E_0^1 + \sum_{n=1}^{N} \rho_n E_n^1 = \sum_{n=0}^{M} (t_n + R_n e^{-\gamma_c^n 1})E_n^2 \quad (11)$$

$$(1-\rho_0)H_0^1 + \sum_{n=1}^{N} \rho_n H_n^1 = \sum_{n=0}^{M} (t_n + R_n e^{-\gamma_c^n 1})H_n^2 \quad (12)$$

$z = 1$

$$\sum_{n=0}^{M} (t_n e^{-\gamma_c^n 1} + R_n)E_n^2 = \sum_{n=0}^{N} T_n E_n^1 \quad (13)$$

$$\sum_{n=0}^{M}(t_n e^{-\gamma_c^n l}-R_n)H_n^2=\sum_{n=0}^{N}T_n H_n^1 \tag{14}$$

where l is the test sample length, γ_c^n the propagation constant of the nth mode of region 2, M the number of modes taken in the region 2 and N the number of modes taken in the region 1 and the region 1′.

Using (11)–(14) and the orthogonality of the modes, the coupling coefficients ρ_n, t_n, R_n, T_n can be related to each other in the following manner

$$\begin{aligned}
&t_i(P_{22}(i)P_{21}^*(i,0)+P_{22}^*(i)P_{12}(i,0))\\
&\quad+R_i e^{-\gamma_c^i l}(P_{22}(i)P_{21}^*(i,0)-P_{22}^*(i)P_{12}(0,i))\\
&\quad=2P_{12}(0,i)P_{21}^*(i,0)+\sum_{n=1}^{N}\rho_n(P_{12}(n,i)P_{21}^*(i,0)\\
&\quad-P_{21}^*(i,n)P_{12}(0,i)) \qquad i=0,\cdots,M
\end{aligned} \tag{15}$$

$$\begin{aligned}
&T_i(P_{11}(i)P_{12}^*(i,0)+P_{11}^*(i)P_{21}(0,i))\\
&\quad=2t_0e^{-\gamma_c^0 l}P_{21}(0,i)P_{12}^*(i,0)\\
&\quad+\sum_{n=1}^{N}[t_n e^{-\gamma_c^n l}(P_{21}(n,i)P_{12}^*(i,0)\\
&\quad+P_{12}^*(i,n)P_{21}(0,i))+R_n(P_{21}(n,i)P_{12}^*(i,0)\\
&\quad-P_{12}^*(i,n)P_{21}(0,i))] \qquad i=0,\cdots,N
\end{aligned} \tag{16}$$

$$R_i=\frac{\sum_{n=0}^{N}T_n(P_{12}(n,i)P_{22}^*(i)-P_{21}^*(i,n)P_{22}(i))}{2P_{22}(i)P_{22}^*(i)} \qquad i=0,\cdots,M \tag{17}$$

$$\begin{aligned}
\rho_i=&\frac{1}{2P_{11}(i)P_{11}^*(i)}\sum_{n=0}^{M}[t_n(P_{21}(n,i)P_{11}^*(i)\\
&-P_{12}^*(i,n)P_{11}(i))+R_n e^{-\gamma_c^n l}(P_{21}(n,i)P_{11}^*(i)\\
&+P_{12}^*(i,n)P_{11}(i))] \qquad i=0,\cdots,N
\end{aligned} \tag{18}$$

with

$$\begin{aligned}
P_{21}(i,j)&=\langle H_j^1|E_i^2\rangle\\
&=\tfrac{1}{2}\int_s[\vec{E}_i^2\wedge\vec{H}_j^1]\cdot d\vec{S}\\
&=\tfrac{1}{2}\int_0^h\int_{-L/2}^{+L/2}[E_{i_x}^2H_{j_y}^{1^*}-H_{j_x}^{1^*}E_{i_y}^2]\,dx\,dy
\end{aligned}$$

and

$$\begin{aligned}
P_{12}(i,j)&=\langle H_j^2|E_i^1\rangle \quad P_{12}^*(i,j)=\langle E_i^1|H_j^2\rangle\\
P_{11}(i)&=\langle H_i^1|E_i^1\rangle \quad P_{11}^*(i)=\langle E_i^1|H_i^1\rangle\\
P_{22}(i)&=\langle H_i^2|E_i^2\rangle \quad P_{22}^*(i)=\langle E_i^2|H_i^2\rangle
\end{aligned}$$

where S is the cross section of the microstrip line and * denotes complex conjugate.

The method chosen to solve the equations (15)–(18) is the Neumann's method [22]. This iterative method consists at first in calculating the initial values of ρ_n, t_n, R_n, T_n neglecting the reflection coefficients of the higher order modes in (15)–(18). Secondly, the values of ρ_n, t_n, R_n, T_n are calculated without approximation from their initial values using (15), (16), (17), (18) and so on, until the convergence of the calculated value of the reflection coefficient of the dominant mode is obtained. Finally, the S-parameters of the microstrip cell are given by

$$S_{11}=S_{22}=\rho e^{-2\gamma_0 l_0}$$
$$S_{21}=S_{12}=Te^{-2\gamma_0 l_0}$$

where γ_o is the propagation constant of the dominant mode of region 1 and region 1′ and l_o the region 1 and region 1′ length.

The numerical computation of the S-parameters of the microstrip cell calls for the truncation of mode sums to a finite number of terms in (15)–(18). We have studied the convergence of the calculated values of the S-parameters as the number of modes taken into account in each region of the

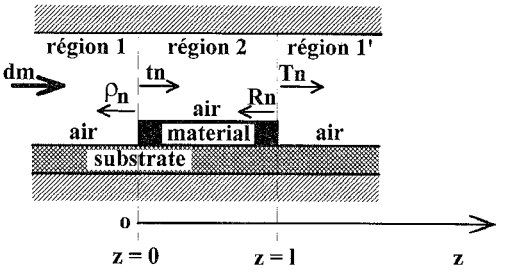

Fig. 9. Unloaded/loaded line discontinuities in the microstrip cell.

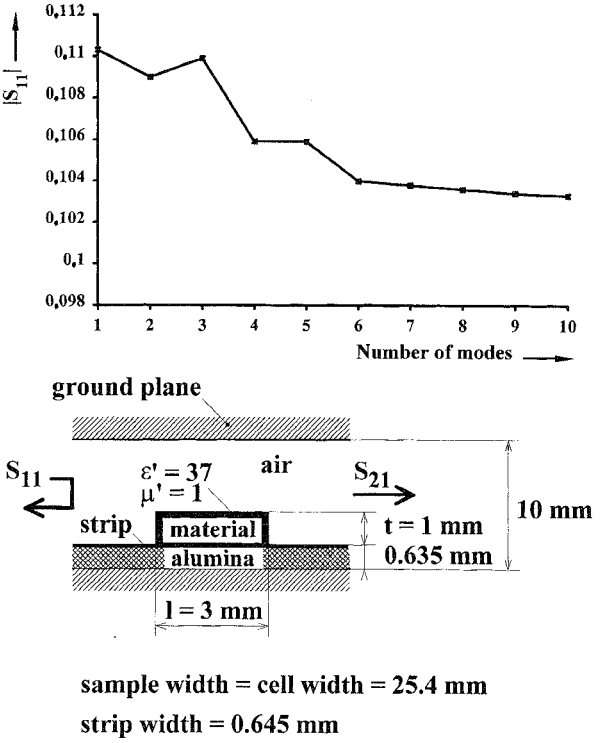

Fig. 10. Convergence of the reflection coefficient modulus as the number of modes taken into account in each region of the microstrip cell (frequency = 1 GHz).

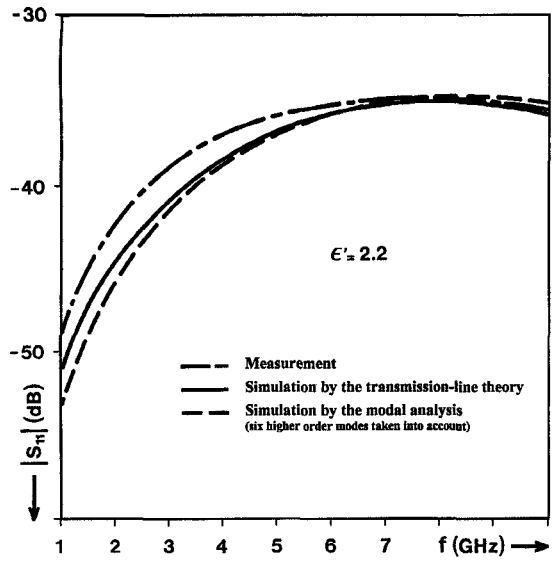

Fig. 11. Variation of the reflection coefficient modulus of the microstrip cell loaded with a low-loss dielectric ($\varepsilon' = 2.2$, sample length $l = 3.2$ mm, thickness $t = 1.5$ mm).

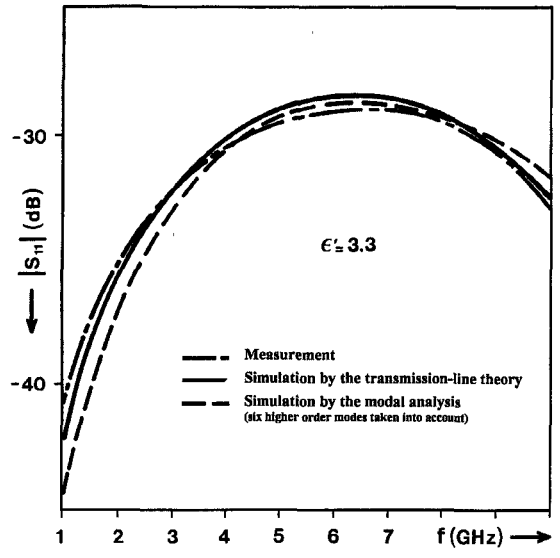

Fig. 12. Variation of the reflection coefficient modulus of the microstrip cell loaded with a low-loss dielectric ($\varepsilon' = 3.3, l = 4$ mm, $t = 2.8$ mm).

cell. Fig. 10 shows that we can typically truncate the mode sums after about ten terms to obtain the accurate calculation of the S-parameters of the cell.

C. Numerical Results and Experimental Verifications

In order to know the influence of the higher order modes on the S-parameters of the microstrip cell and the domain of validity of the transmission-line theory previously used [1], we have compared the simulated S-parameters to the measured S-parameters, on one hand, and to the S-parameters calculated from the transmission-line theory, on the other hand. Fig. 11–13 show the results obtained for three discontinuities using different materials. In order to make the comparisons between theoretical and experimental results easier, we have chosen dielectric materials with well-known properties and a relative

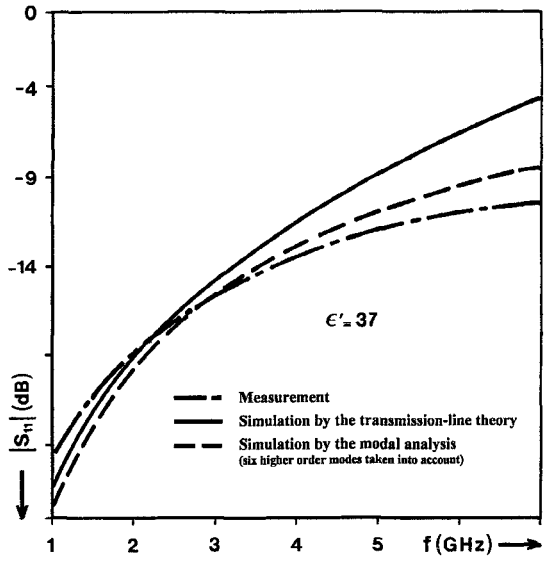

Fig. 13. Variation of the reflection coefficient modulus of the microstrip cell loaded with a low-loss dielectric ($\varepsilon' = 37, l = 2$ mm, $t = 1$ mm).

permittivity which is constant in the exploited frequency band. For the discontinuities using a dielectric material with a low dielectric constant ($\varepsilon' = 2.2$ and $\varepsilon' = 3.3$), the simulated values of the reflection coefficient modulus in Fig. 11 and Fig. 12 are in close agreement over the exploited frequency band with the measured values and those obtained with the transmission-line theory. On the contrary, for the dielectric material with a great dielectric constant ($\varepsilon' = 37$), the gap between the measured values and those obtained with the transmission-line theory widens as the frequency increases, while the values simulated by the modal analysis are closer to the measurements with only six higher order modes taken into account on both sides of each loaded/unloaded line discontinuity (Fig. 13). These results confirm the influence of the higher order modes of the microstrip line on the S-parameters of the cell. They also prove that when the transmission-line theory is used to describe the electromagnetic behavior of the cell discontinuities, the results previously obtained are worse at high frequencies for materials with great electric and magnetic susceptibilities.

V. Conclusion

We have previously developed a method easy to implement for the broad band measurement of the complex permittivity and permeability of materials [1]. This method is based on the reflection/transmission measurement of a microstrip line loaded with the test sample. The fact that the measurement results on materials were worse in high frequencies for samples with great values of electric and magnetic susceptibilities over the exploited frequency band, brought us to study the domain of validity of the transmission-line theory used to describe the electromagnetic behavior of the unloaded/loaded line discontinuities during the processing of the data. In this paper, we have presented the rigorous analysis of the microstrip cell discontinuity taking into account the higher order modes that can be excited at the discontinuities. We have shown the influence of these modes on the S-parameters of the cell. For materials

with low electromagnetic characteristics (typically $\varepsilon' < 10$ and $\mu' < 10$ over about 6 GHz) in the cell, the transmission-line theory is in close agreement with the measurements in the exploited frequency band (45 MHz–14 GHz). On the other hand, for materials with greater permittivity and permeability in high frequencies, higher order modes must be taken into account in the calculations of the S-parameters of the cell. In this case, the modal analysis (modal matching at the cell discontinuities) must replace the transmission-line theory to describe rigorously the electromagnetic behavior of the cell discontinuities in the processing of the data. The resolution of the inverse problem is more difficult when higher order modes are calculated in the direct problem. As a consequence, in this paper we have only considered the direct problem. The study of a new numerical method for the calculation of higher order modes at the time of the resolution of the inverse problem will be presented in a future paper.

REFERENCES

[1] P. Queffelec, P. Gelin, J. Gieraltowski, and J. Loaec, "A microstrip device for the broad-band simultaneous measurement of complex permeability and permittivity," *IEEE Trans. Magn.*, vol. 30, no. 2, pp. 224–231, Mar. 1994.

[2] W. B. Weir, "Automatic measurement of complex dielectric constants and permeability at microwave frequencies," *Proc. IEEE*, vol. 62, no. 1, pp. 33–36, Jan. 1974.

[3] W. Barry, "A broad-band, automated, stripline technique for the simultaneous measurement of complex permittivity and permeability," *IEEE Trans. Microwave Theory Tech.*, vol. MTT-34, no. 1, pp. 80–84, Jan. 1986.

[4] S. Li, C. Akyel, and R. G. Bosisio, "Precise calculation and measurements on the complex dielectric constant of lossy material TM_{010} using cavity perturbation techniques," *IEEE Trans. Microwave Theory Tech.*, vol. MTT-29, pp. 1041–1048, 1981.

[5] G. Engen and C. Hoer, "Thru-Reflect-Line: An improved technique for calibrating the dual six-port automatic network analyzer," *IEEE Trans. Microwave Theory Tech.*, vol. MTT-27, no. 12, pp. 987–993, Dec. 1979.

[6] R. Mittra and T. Itoh, "A new technique for the analysis of the dispersion characteristics of microstrip lines," *IEEE Trans. Microwave Theory Tech.*, vol. MTT-19, no. 1, pp. 54–63, Jan. 1971.

[7] T. Itoh and R. Mittra, "Spectral-domain approach for calculating the dispersion characteristics of microstrip lines," *IEEE Trans. Microwave Theory Tech.*, vol. MTT-21, pp. 407–409, July 1973.

[8] R. H. Jansen, "The spectral-domain approach for microwave integrated circuits," *IEEE Trans. Microwave Theory Tech.*, vol. MTT-33, no. 10, pp. 1043–1056, Oct. 1985.

[9] A. Globus, V. Cagan, H. Pascard, M. Le Floc'h, and J. Loaec, "Coherence of magnetic phenomena in ferrimagnetic materials as a function of spin and domain wall topography," Ferrites: Proc. Int. Conf., Sept.-Oct. 1980, Japan.

[10] J. Esteban and J. M. Rebollar, "Characterization of corrugated waveguides by modal analysis," *IEEE Trans. Microwave Theory Tech.*, vol. 39, no. 6, pp. 937–943, June 1991.

[11] L. Carin, K. J. Webb, and S. Weinred, "Matched windows in circular waveguide," *IEEE Trans. Microwave Theory Tech.*, vol. 36, pp. 1359–1362, no. 9, Sept. 1988.

[12] K. C. Gupta, R. Gary, and I. J. Bahl, *Microstrip Lines and Slotlines*. Norwood, MA: Artech House, 1979.

[13] T. Itoh, "Spectral domain immitance approach for dispersion characteristics of generalized printed transmission lines", *IEEE Trans. Microwave Theory Tech.*, vol. MTT-28, no. 7, pp. 733–736, July 1980.

[14] P. Quéffélec, "Conception d'une cellule microruban pour la mesure large bande (45 MHz - 12 GHz) de la permittivité et de la perméabilité complexes des matériaux. Application à la caractérization électromagnétique des couches minces dans le domaine des micro-ondes", thèse de Doctorat nouveau régime, Université de Bretagne Occidentale, Brest, Octobre 1994.

[15] R. Mittra, T. Itoh, and T. S. Li, "Analytical and numerical studies of the relative convergence phenomenon arising in the solution of an integral equation by the moment method," *IEEE Trans. Microwave Theory Tech.*, vol. MTT-20, pp. 96–104, Feb. 1972.

[16] M. Leroy, "On the convergence of numerical results in model analysis," *IEEE Trans. Antennas Propagat.*, vol. 31, pp. 656–659, July 1983.

[17] C. J. Railton and T. Rozzi, "Complex modes in boxed microstrip," *IEEE Trans. Microwave Theory Tech.*, vol. 36, no. 5, pp. 865–874, May 1988.

[18] D. E. Muller, "A method for solving algebraic equations using an automatic computer," *Mathematical Tables and Aids to Computation*, vol. 10, pp. 208–215, 1956.

[19] F. G. Curtis and P. O. Wheatley, *Applied Numerical Analysis*. Reading, MA: Addison-Wesley.

[20] F. Huret, "Etude comparative de l'Approche dans le Domaine Spectral et de la méthode des Equations Intégrales Singulières pour la simulation des lignes planaires en technologie monolithique microonde", Thèse de Doctorat Nouveau Régime, Université des Sciences et Technologies de Lille. Décembre 1991.

[21] W. X. Huang and T. Itoh, "Complex modes in lossless shielded microstrip lines," *IEEE Trans. Microwave Theory Tech.*, vol. 36, no. 1, pp. 163–165, Jan. 1988.

[22] P. Gelin, "Traitement électromagnétique des discontinuités en guides d'ondes diélectriques: Application aux résonateurs diélectriques", Thèse de Doctorat d'Etat, Septembre 1981, Université des Sciences et Techniques de Lille.

Patrick Quéffélec was born on December 7, 1966, in Quimper, France. He received the doctor in electronics degree from the Université de Bretagne Occidentale, Brest, France, in 1994.

Presently, he is Assistant Professor at the Université de Bretagne Occidentale. His research activities concern with electromagnetic wave propagation in heterogeneous materials and the analysis of methods for microwave measurement of complex permittivity and permeability.

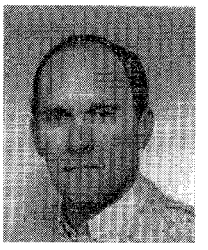

Philippe Gelin was born on June 1, 1948, in St. Avold, France. He received the doctor in physics degree from the Technical University of Lille, France, in 1981.

Presently, he is Professor of Electrical Engineering at the Ecole Nationale Supérieure des Télécommunications de Bretagne, Brest, in the Laboratoire d'Etudes des Systèmes de Télécommunciations (LEST, URA CNRS no. 1329).